Integrated Diamond Networks for Quantum Nanophotonics

Communication

Integrated diamond networks for quantum nanophotonics

Birgit J. M. Hausmann, Brendan Shields, Qimin Quan, Patrick Maletinsky, Murray McCutcheon, Jennifer T Choy, Tom M. Babinec, Alexander Kubanek, Amir Yacoby, Mikhail D. Lukin, and Marko Loncar

Nano Lett., **Just Accepted Manuscript** • Publication Date (Web): 16 Feb 2012

Integrated diamond networks for quantum nanophotonics

Birgit J.M. Hausmann[1], Brendan Shields[2], Qimin Quan[1], Patrick Maletinsky[2], Murray McCutcheon[1], Jennifer T. Choy[1], Tom M. Babinec[1], Alexander Kubanek[2], Amir Yacoby[2], Mikhail D. Lukin[2], Marko Lončar[1]*

1. Harvard University, School of Engineering and Applied Sciences, 33 Oxford Street, Cambridge, USA and

2. Harvard University, Department of Physics, 17 Oxford Street, Cambridge, USA

ABSTRACT: We demonstrate an integrated nanophotonic network in diamond, consisting of a ring resonator coupled to an optical waveguide with grating in- and outcouplers. Using a Nitrogen-Vacancy color center embedded inside the ring resonator as a source of photons, single photon generation and routing at room temperature is observed. Furthermore, we observe a large overall photon extraction efficiency (10%) and high quality factors of ring resonators (3,200 for waveguide-coupled system and 12,600 for a bare ring).

KEYWORDS: Nitrogen-vacancy (NV) center, diamond, photonic crystal cavity, single photon source, cavity QED, on-chip photonics.

For applications in quantum information science and technology, diamond offers unique advantages over other solid-state platforms. The existence of luminescent defects such as Nitrogen Vacancy (NV) centers, that can be used as a long-lived (spin-based) memory with optical read-out, makes diamond a promising platform for quantum information processing (QIP)[1–3]. In particular, NV centers coupled to a resonator could form a quantum node of a quantum network to store, manipulate and process information while waveguides could represent quantum channels between the nodes that transfer quantum information[3,4]. While proof-of-principle quantum networks with diamond NV centers have previously been demonstrated[5,6], the scalability of the approach crucially depends on the realization of an integrated diamond nanophotonic platform. Until recently scalable diamond photonics has been limited to bulk[7–12] or polycrystalline diamond devices[13–15] due to difficulties associated with the fabrication of thin, single crystal, diamond (SCD) films on sacrificial or low index substrates. Light absorption and scattering at grain boundaries can be detrimental for the polycrystalline diamond approaches, while the realization of scalable, on-chip quantum networks is challenging with single-crystal bulk diamond approaches. Here, we demonstrate the building block of an all-diamond photonic network on chip that overcomes these issues, and represents a leap forward for quantum optics applications. The node of the network consists of a single NV center coupled to the mode of a high-Q ring resonator and a low loss waveguide that is evanescently coupled to the cavity could be used as a routing element between nodes.

Our approach involves the fabrication of high quality, low loss ring resonators directly in single crystal diamond (SCD) thin slabs. Figure 1a illustrates our fabrication sequence, based on the approach that we[16,17] as well as others[18] have recently demonstrated. First we thin a 20 μm thick type Ib single crystal diamond slab (Element Six) to the preferred device layer thickness by an oxygen-based inductively coupled reactive ion etch (ICP RIE)[19]. An e-beam (Elionix) exposes XR e-beam resist (spin-on-glass, Dow Corning) to form a mask which we transfer to the diamond film in a second etch. Figure 1b shows a scanning electron microscope (SEM) image of representative diamond ring resonators, with different diameter and ring cross-sectional dimensions, on SiO_2/Si substrate.

In order to characterize our diamond resonators we take advantage of the intrinsic fluorescence of embedded color centers. We use a photoluminescence approach in a scanning confocal microscope using two collection arms[20](Fig. 1 and Methods). Green pump light (532 nm) scans the devices at normal incidence (Fig. 1c) via a scanning mirror, and red photons (650 nm-800 nm) emitted from NV centers are collected and analyzed after passing through a dichroic mirror (DM) and longpass filters. Our detection path is split into two arms, one of which is always fixed at the excitation spot (C1) while the second arm can be scanned independently (C2). The latter allows us to spatially separate excitation and collection positions. First, we scan the sample to obtain an emission image of the device using C1. Figure 1c(right), shows a scan of the photon collection position over the ring in C2 (yellow circle) while constantly exciting with the pump laser in the same position (red circle). The device shown in the figure has an outer ring radius of 20 μm and a 1 μm × 410 nm cross-section with 300 nm XR covering the diamond. The intensity profile of the ring indicates excitation of a higher order mode (confirmed by 3-D finite difference time domain (FDTD) simulations, not shown). The spectrum reveals multimode behavior of the cavity with quality (Q) factors of $Q \approx 12,600$ and a finesse F of 62 (Fig. 1d and inset).

To form a node of a network it is necessary to integrate the ring resonator with a channel that carries information. We monolithically fabricate ring resonators next to optical waveguides and thereby provide efficient and robust in- and outcoupling of light to the resonator with embedded single NV centers. The waveguides contain second order gratings on each end to facilitate free-space coupling of photons (Fig. 2a). We characterize the structure by coupling the light from a broadband white light source into one grating and by collecting transmitted light from the other grating. The transmission spectrum shows regularly spaced dips corresponding to the different (longitudinal) resonant modes of the ring resonator (Fig. 2b). We extract a Q-factor of $Q \approx 2500$ and $F \approx 40$ for the resonance at $\lambda = 689.8$ nm. Here,

we operate close to critical coupling where the decay rate to the waveguide would equal the intrinsic field decay rate of the resonator.

Additionally, we demonstrate efficient generation and routing of nonclassical light fields provided by a single NV center embedded inside the diamond ring resonator, at room temperature. Single photons emitted from the NV center into the ring resonator couple evanescently to the waveguide and are outcoupled one by one by the gratings. Figure 3a) and b) illustrate scans using the two confocal collection channels C1 and C2, respectively (the device is different from the one shown in Fig. 2). We excite an NV center with green light (532 nm) and use collection arm C_2 to collect photons from three different locations: directly above the NV center - denoted by C_{21}, and from both grating couplers - C_{22} for the coupler on the left, and C_{23} for the one on the right. Collection arm C_1, positioned above the NV center, is used to collect photons emitted directly by the NV center - denoted by C_{11}. We use Hanbury Brown and Twiss (HBT) configuration[21] to evaluate the second-order intensity correlations $g^{(2)}(\tau)$ where nonclassical light behavior from a single quantum emitter results in $g^{(2)}(0) < 0.5$[22]. First we study the free-space emission of the NV center (Fig. 3d). Here, light is directly emitted upwards and extracted at the pump position in each collection position (C_{11} and C_{21}). The cross-correlation between C_{11} and C_{21} shows strong photon antibunching demonstrating the single photon character of the emitted quantum field. The increased coincidence rate for $12\,\text{ns} < \tau < 550\,\text{ns}$ is attributed to an intermediate shelving state, characteristic of an NV center's emission[23]. When collecting photons emitted directly above the NV center (combining C_{11} and C_{21}) we observe the typical NV center's emission spectrum (Fig. 3g) where the majority of collected photons are emitted directly into the free-space without coupling into the ring modes. Furthermore, the Raman line occurs at the same spectral position (573 nm) as in bulk diamond, indicating a good film quality (Fig. 3, as denoted by R in all spectra). The spectra at the outcoupling gratings (Fig. 3f and 3h) feature prominent peaks indicating coupling of the NV center's fluorescence to the modes of the ring resonator as well as transfer of emitted photons into the waveguide. Based on this fluorescence spectrum we measure loaded Q-factors as high as $(3.2 \pm 0.4) \cdot 10^3$ at 665.9 nm. Moreover, we observe the evidence of routing of the quantum light field when we cross-correlate C_{11} with C_{22} and C_{23}. We confirm strong photon antibunching without significant change of the light statistics compared to the auto-correlated free-space emission (Fig. 3 c) and 3 e), respectively).

Finally, we evaluate the performance of the routing process by comparing the saturation behavior of the NV center emission into free space with its emission into the photonic structure. We obtain the net count rate by subtracting the background (linearly increasing with pump power) from the overall counts and fit according to[23]: $I(P) = \frac{\mathrm{I_{Sat}}}{1+\mathrm{P_{Sat}}/\mathrm{P}}$ where $\mathrm{I_{Sat}}$, $\mathrm{P_{Sat}}$ are the saturated count intensity and pump power, respectively. The free space emission of the NV center, obtained by adding $\mathrm{C_{11}}$ and $\mathrm{C_{21}}$, saturates at a count level of $(15 \pm 0.2) \cdot 10^4$ counts per seconds (CPS) at a pump power of $(120 \pm 7)\,\mu\mathrm{W}$. This saturation level is significantly higher when compared to an NV center in bulk which we attribute to a thin film effect[24] combined with the NV center's polarization-dependent coupling to the ring. At the same time, the combined counts from the outcoupling gratings give $(15 \pm 0.1) \cdot 10^3$ CPS at saturation at a pump power of $(100 \pm 4)\,\mu\mathrm{W}$. Using 3-D FDTD modeling we estimate the overall collection efficiency of our current grating design to be 30 %. In addition, by modeling the coupling efficiency from the NV center to the ring and from the ring to the waveguide we estimate a total collection efficiency of our system to be 15 % - that is 15 % of photons emitted by an NV center are outcoupled by the gratings and collected using our collection optics. We note that reduced photon counts collected from gratings are largely due to the confocal nature of our experimental apparatus which collects light only from a small ($< 1\,\mu\mathrm{m}^2$) region of the grating. The collection from the gratings could be significantly improved if light from the whole grating regions is collected using a multimode fiber or an objective lens. Improvements in the design of the gratings themselves can increase the collection efficiency up to 90 %[25]. Finally, inverse-taper waveguide outcoupling[26,27] could be used to efficiently collect most of the emitted light directly from the waveguide, without a need for a grating.

Our first demonstration of an integrated on-chip optical network based on diamond illustrates the great potential of a diamond-on-insulator platform in the field of quantum optics. The compact architecture and low loss material make our diamond platform suitable for large scale integration where multiple devices can be connected via single photon channels, thus enabling on-chip photonic networks. With the recent progress of spin-photon entanglement with single NV centers[28] our approach may pave the way for the realization of integrated, scalable quantum networks[4] in which photons are used to transfer quantum information between different nodes (e.g. NV center embedded inside cavity) of the network. Due to their long spin coherence times at room temperature, NV centers are not only promising candidates for quantum memory, but also have intriguing applications in quantum sensing[19,29,30]. In order to enhance the interaction between light and an NV center, and possibly enter the strong-coupling regime of light-matter interaction, photonic crystal cavities fabricated directly in diamond will be explored. Besides other applications, entering the strong coupling regime could be applied to realize single photon transistors[31,32] based on diamond.

Supporting Information Available. A more detailed description of the confocal microscope setup containing two collection arms as well as 3D FDTD modeling on the coupling efficiency, mode volume and Purcell effect of our device is provided in the supporting information section. This material is available free of charge via the Internet at

http://pubs.acs.org.

I. ACKNOWLEDGEMENTS

Devices were fabricated in the Center for Nanoscale Systems (CNS) at Harvard. The authors thank Parag Deotare for many helpful discussions and Daniel Twitchen and Matthew Markham from Element Six for support with diamond samples. T.M.B. was supported by the NDSEG and the NSF graduate student fellowships, and J.T.C. by the NSF graduate student fellowship. A.K. acknowledges support from the Alexander von Humboldt Foundation. This work was supported in part by the National Science Foundation (NSF) Nanotechnology and Interdisciplinary Research Team grant (ECCS-0708905), the Defense Advanced Research Projects Agency (Quantum Entanglement Science and Technology program), and the Hewlett Packard Foundation as well as AFOSR MURI (grant FA9550-09-1-0669-DOD35CAP). M.L. acknowledges support from the Sloan Foundation.

II. AUTHOR INFORMATION

Correspondence and requests for materials should be addressed to M.L. (email: loncar@seas.harvard.edu)

[1] Wrachtrup, J.; Jelezko, F. *J. Phys.: Condens. Matter* **2006**, *18*, 807–824.
[2] Neumann, P.; Mizuochi, N.; Rempp, F.; Hemmer, P.; Watanabe, H.; Yamasaki, S.; Jacques, V.; Gaebel, T.; Jelezko, F.; Wrachtrup, J. *Science* **2008**, *320*, 1326.
[3] O'Brien, J. L. *Science* **2007**, *318*, 1567.
[4] Kimble, H. J. *Nature* **2008**, *453*, 1023–1030.
[5] Childress, L.; Taylor, J. M.; Sørensen, A. S.; Lukin, M. D. *Phys. Rev. Lett.* **2006**, *96*, 070504.
[6] Beveratos, A.; Brouri, R.; Gacoin, T.; Villing, A.; Poizat, J. P.; Grangier, P. *Phys. Rev. Lett* **2002**, *89*, 187901.
[7] Aharonovich, I.; Greentree, A. D.; Prawer, S. *Nature Photon.* **2011**, *5*, 397.
[8] Babinec, T.; Hausmann, B. M.; Khan, M.; Zhang, Y.; Maze, J.; Hemmer, P. R.; Loncar, M. *Nature Nanotech.* **2010**, *5*, 195–199.
[9] Hadden, J. P.; Harrison, J. P.; Stanley-Clarke, A. C.; Marseglia, L.; Ho, Y.-L. D.; Patton, B. R.; OŠBrien, J. L.; Rarity, J. G. *Appl. Phys. Lett.* **2010**, *97*, 241901.
[10] Siyushev, P.; Kaiser, F.; Jacques, V.; Gerhardt, I.; Bischof, S.; Fedder, H.; Dodson, J.; Markham, M.; Twitchen, D.; Jelezko, F.; Wrachtrup, J. *Appl. Phys. Lett.* **2010**, *97*, 241902.
[11] Choy, J. T.; Hausmann, B. J. M.; Babinec, T. M.; Bulu, I.; Khan, M.; Maletinsky, P.; Yacoby, A.; Loncar, M. *Nature Photon.* **2011**, *5*, 738, Submitted.
[12] Barclay, P. E.; Fu, K.-M. C.; Santori, C.; Beausoleil, R. G. *Appl. Phy. Lett.* **2009**, *95*, 191115.
[13] Wang, C. F.; Choi, Y.-S.; Lee, J. C.; Hu, E. L.; Yang, J.; Butler, J. E. *Appl. Phy. Lett.* **2007**, *90*, 081110.
[14] Wang, C. F.; Hanson, R.; Awschalom, D. D.; Hu, E. L. *Appl. Phy. Lett.* **2007**, *91*, 201112.
[15] Hiscocks, M. P.; Ganesan, K.; Gibson, B. C.; Huntington, S. T.; Ladouceur, F.; Prawer, S. *Opt. Express* **2009**, *16 (24)*, 19512–19519.
[16] Loncar, M.; Babinec, T.; Choy, J.; Hausmann, B.; Bulu, I.; Zhang, Y.; Khan, M.; McCutcheon, M. W. Diamond Nanophotonics and Quantum Optics. *Artificial Atoms in Diamond: From Quantum Physics to Applications*, Cambridge, USA, 2010.
[17] Hausmann, B.; Choy, J.; Quan, Q.; McCutcheon, M.; Maletinsky, P.; Babinec, T.; Chu, Y.; Kubanek, A.; Yacoby, A.; Lukin, M.; Loncar, M. On-Chip single crystal diamond resonators. *CLEO/QELS 2011*, Baltimore, USA, 2011.
[18] Faraon, A.; Barclay, P. E.; Santori, C.; Fu, K.-M. C.; Beausoleil, R. G. *Nature Photon.* **2010**, *5*, 301–305.
[19] Maletinsky, P.; Hong, S.; Grinolds, M.; Hausmann, B.; M.D.Lukin,; Walsworth, R.-L.; Loncar, M.; Yacoby, A. arXiv:1108.4437.
[20] Akimov, A. V.; Mukherjee, A.; Yu, C. L.; Chang, D. E.; Zibrov, A. S.; Hemmer, P. R.; Park, H.; Lukin, M. D. *Nature* **2007**, *450*, 402–406.
[21] Brown, R. H.; Twiss, R. Q. *Nature* **1956**, *177*, 27–29.
[22] Kimble, H. J.; Dagenais, M.; Mandel, L. *Phys. Rev. Lett.* **1977**, *39*, 691.
[23] Kurtsiefer, C.; Mayer, S.; Zarda, P.; Weinfurter, H. *Phys. Rev. Lett.* **2000**, *85*, 290.
[24] Lee, K. G.; Chen, X. W.; Eghlidi, H.; Kukura, P.; Lettow, R.; Renn, A.; Sandoghdar, V.; Goetzinger, S. *Nature Photon.* **2011**, *5*, 166.
[25] Laere, F. V.; Roelkens, G.; Ayre, M.; Schrauwen, J.; Taillaert, D.; Thourhout, D. V.; Krauss, T. F.; Baets, R. *J. Lightwave Technol.* **2007**, *25 (1)*, 151–156.
[26] Almeida, V. R.; Panepucci, R. R.; Lipson, M. *Opt. Lett.* **2003**, *28 (15)*, 1302–1304.
[27] Shoji, T.; Tsuchizawa, T.; Watanabe, T.; Yamada, K.; Morita, H. *Electron. Lett.* **2002**, *38 (25)*, 1669–1670.

[28] Togan, E.; Chu, Y.; Trifonov, A. S.; Jiang, L.; Maze, J.; Childress, L.; Dutt, M. V. G.; Sørensen, A. S.; Hemmer, P. R.; Zibrov, A. S.; Lukin, M. D. *Nature* **2010**, *466*, 730–734.
[29] Maze, J. R.; Stanwix, P. L.; Hodges, J. S.; Hong, S.; Taylor, J. M.; Cappellaro, P.; Jiang, L.; Dutt, M. V. G.; Togan, E.; Zibrov, A. S.; Yacoby, A.; Walsworth, R. L.; Lukin, M. D. *Nature* **2008**, *455*, 644.
[30] Balasubramanian, G.; Chan, I. Y.; Kolesov, R.; Al-Hmoud, M.; Tisler, J.; Shin, C.; Kim, C.; Wojcik, A.; Hemmer, P. R.; Krueger, A.; Hanke, T.; Leitenstorfer, A.; Bratschitsch, R.; Jelezko, F.; Wrachtrup, J. *Nature* **2008**, *455*, 648–651.
[31] Chang, D. E.; Sørensen, A. S.; Demler, E. A.; Lukin, M. D. *Nat. Phys.* **2007**, *3*, 807–812.
[32] Hwang, J.; Pototschnig, M.; Lettow, R.; Zumofen, G.; Renna, A.; Götzinger, S.; Sandoghdar, V. *Nature* **2009**, *460*, 76–80.

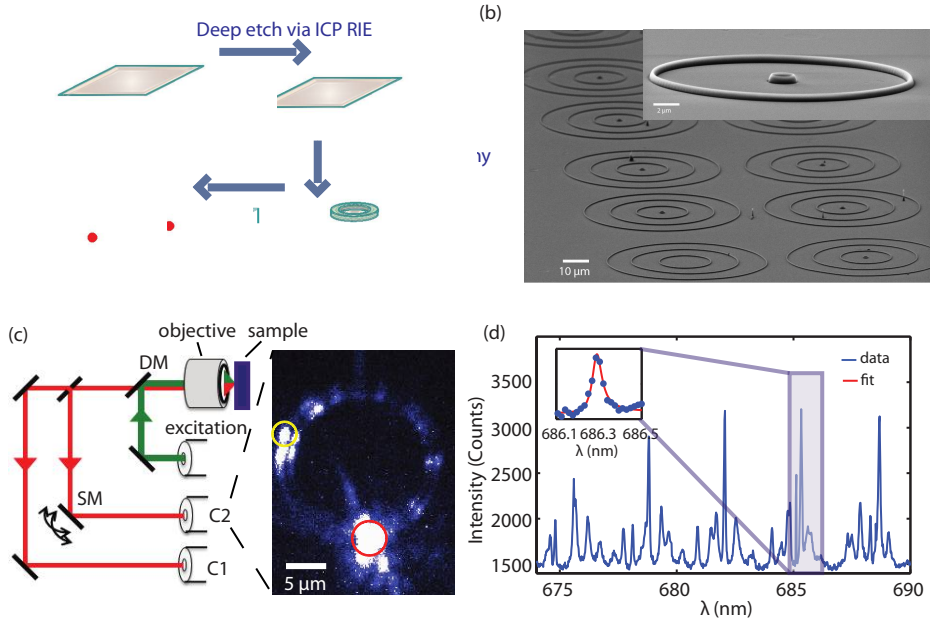

FIG. 1: **(a)** Fabrication schematic used to make ring resonators is as follows: First, we thin a diamond slab via an oxygen based reactive ion etch (RIE). Next we use e-beam lithography to define a the devices in e-beam resist. Finally we transfer the mask into the thinned diamond slab using RIE. Residual resist is not removed from devices during characterization. Optically active defect centers are indicated in red. **(b)** The SEM image shows diamond ring resonators on SiO_2/Si with varying radii. Inset: Higher magnification image of two ring resonators with smooth sidewalls. **(c)** Schematic of a two collection arm confocal microscope. Having obtained a scan of the device using collection arm C_1 we fix the green pump beam (red circle) and use collection arm C_2 to obtain a second scan and collect photons from a different position at the ring resonator (yellow circle). The yellow circle also marks the collection position while taking spectra. **(d)** The photoluminescence spectrum features peaks that correspond to the modes of the resonator. A pump power of 1.5 mW is used at an integration time of 300 s. Inset: A Q-factor of $(12.6 \pm 1) \cdot 10^3$ is obtained by fitting the experimental data (red).

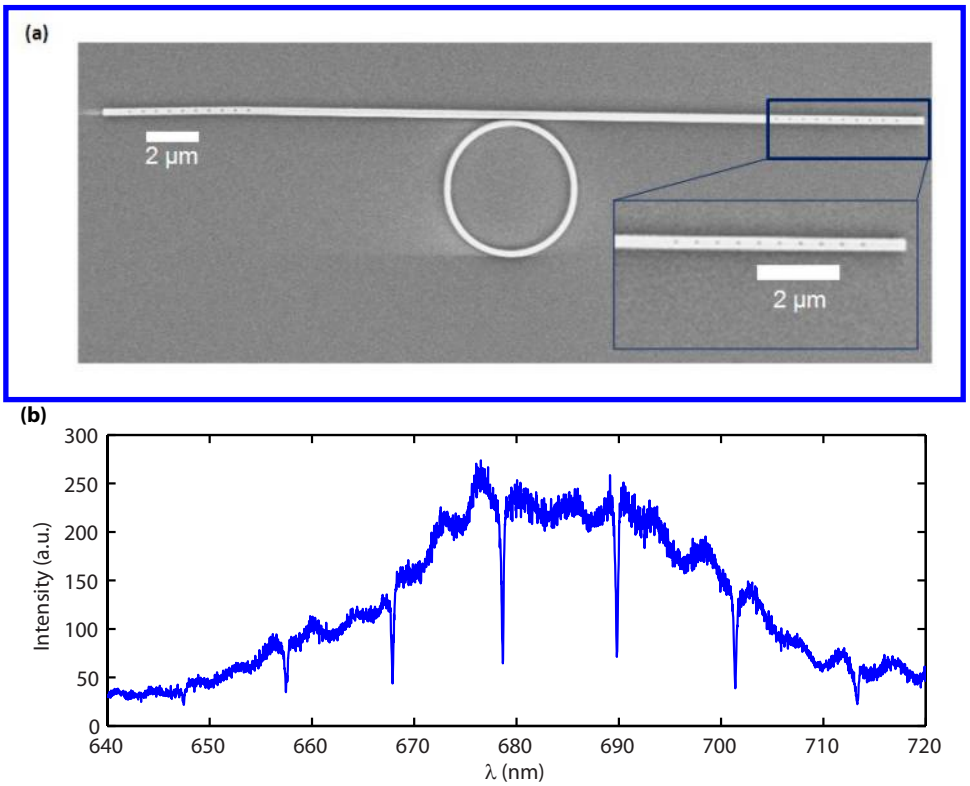

FIG. 2: **(a)** SEM image of a single mode ring resonator coupled to a waveguide containing second order gratings on both ends. The ring diameter is 5 μm and its width is 245 nm. The gap between the waveguide and the ring is 100 nm, while the waveguide itself has a width of 370 nm. The device is sitting on a SiO_2/Si substrate. Inset: Magnified image of the grating region. **(b)** The transmission spectrum is obtained by exciting the structure with white light (from super-continuum source) using the right-hand side grating, and measuring transmitted signal using the left-hand side grating. The dips in the transmission correspond to the ring resonator modes.

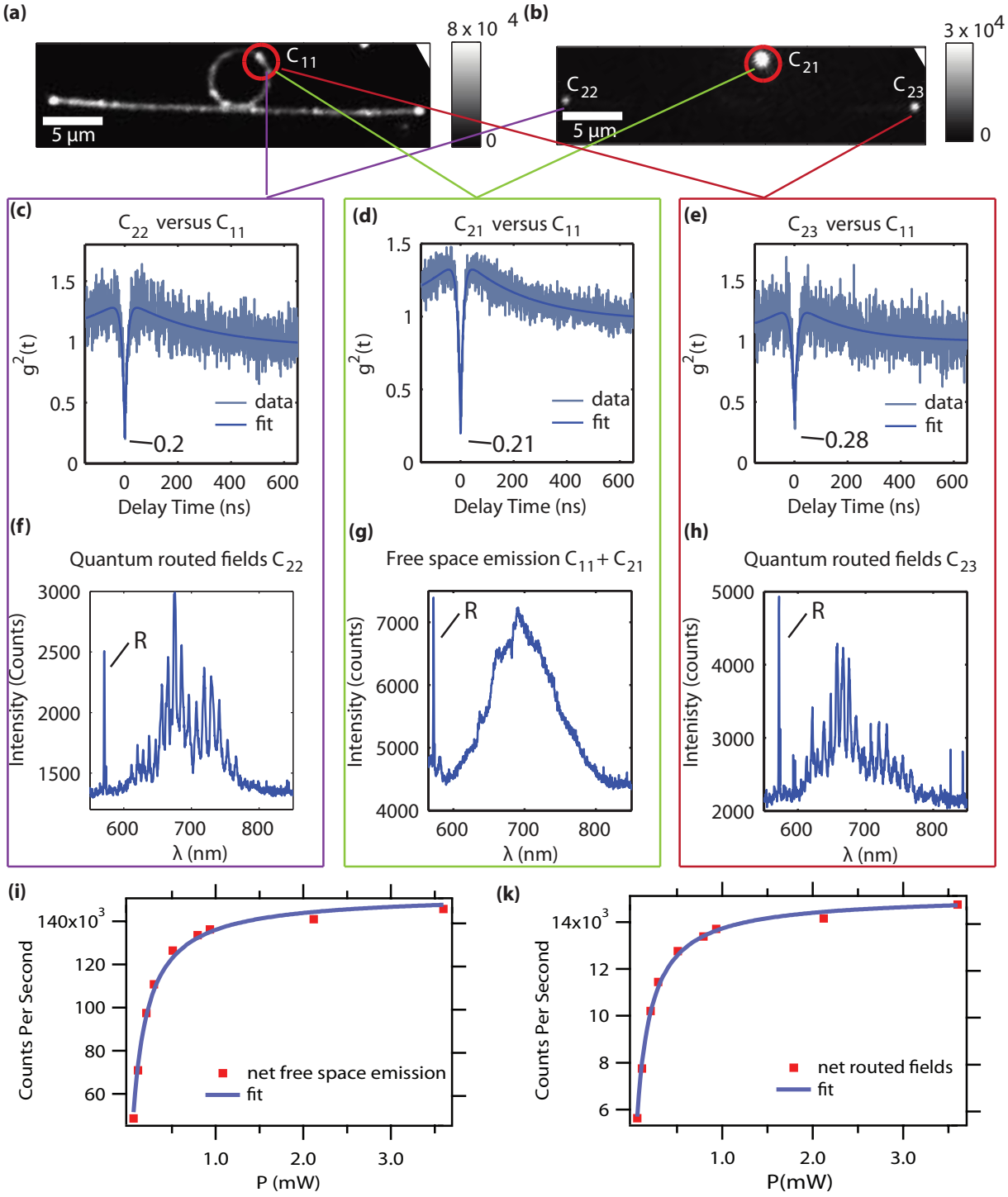

FIG. 3: **(a)** Confocal image of the device is obtained by scanning the pump laser and using collection arm C1 to collect the fluorescence (see also figure 1). After presence of NV center is confirmed, we position the pump beam at its location. **(b)** Second confocal image can then be acquired using the collection arm C2. Furthermore, C2 arm can be used to collect light from three locations of interest: NV center position (C_{21}), left hand side grating (C_{22}) and right hand side grating (C_{23}). **(c-e)** Hanbury-Brown-Twiss apparatus confirms emission and routing of nonclassical light, by cross correlating signals C_{11} with C_{21} as well as C_{23} and C_{22}. Strong anti-bunching ($g^{(2)}(0) < 0.5$) is observed, without any background subtraction. **(g)** The combined spectrum of C_{11} and C_{21} shows the characteristic NV emission. The exact same position of the (non-broadened) Raman line at 573 nm as in the bulk diamond indicates that the single crystal diamond film quality is comparable to bulk diamond (denoted by R). **(f), (h)** Spectra collected from the gratings C_{22}, C_{23}, respectively, reveal resonances of the ring imprinted on the phonon sideband of the NV center's emission (using a 150 lines/mm grating). We obtain a Q-value of $(3.2 \pm 0.4) \cdot 10^3$ for the resonance at 665.9 nm using a large resolution grating (1800 lines/mm). **(i)** Free-space collection exhibits a saturated single photon flux of $(15 \pm 0.2) \cdot 10^4$CPS at a pump power of 120 ± 7 µW from an NV center. The net counts from a single NV center are obtained via subtracting the linear background from the overall count rate. **(k)** The combined count rate at both gratings gives a saturation level of $(15 \pm 0.1) \cdot 10^3$ CPS at a saturation pump power of (100 ± 4) µW.

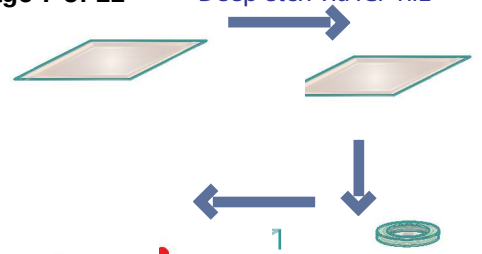

(b)

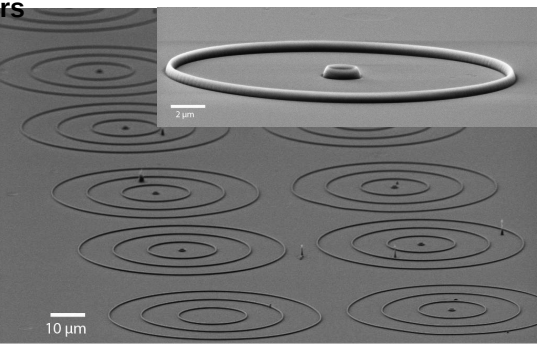

(c)

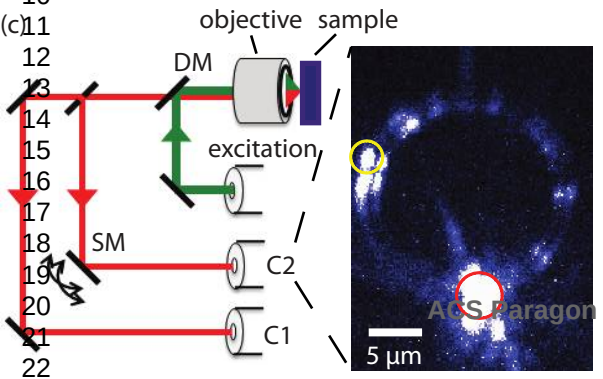

(d)

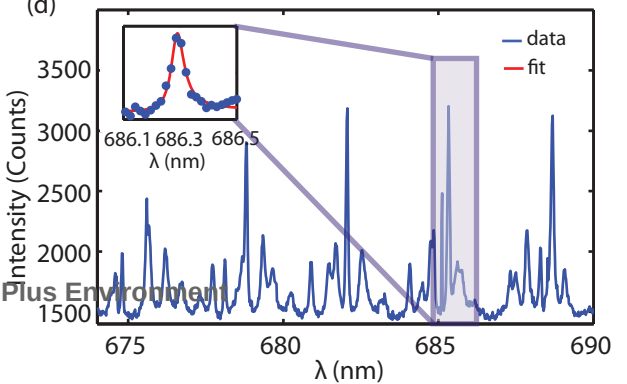

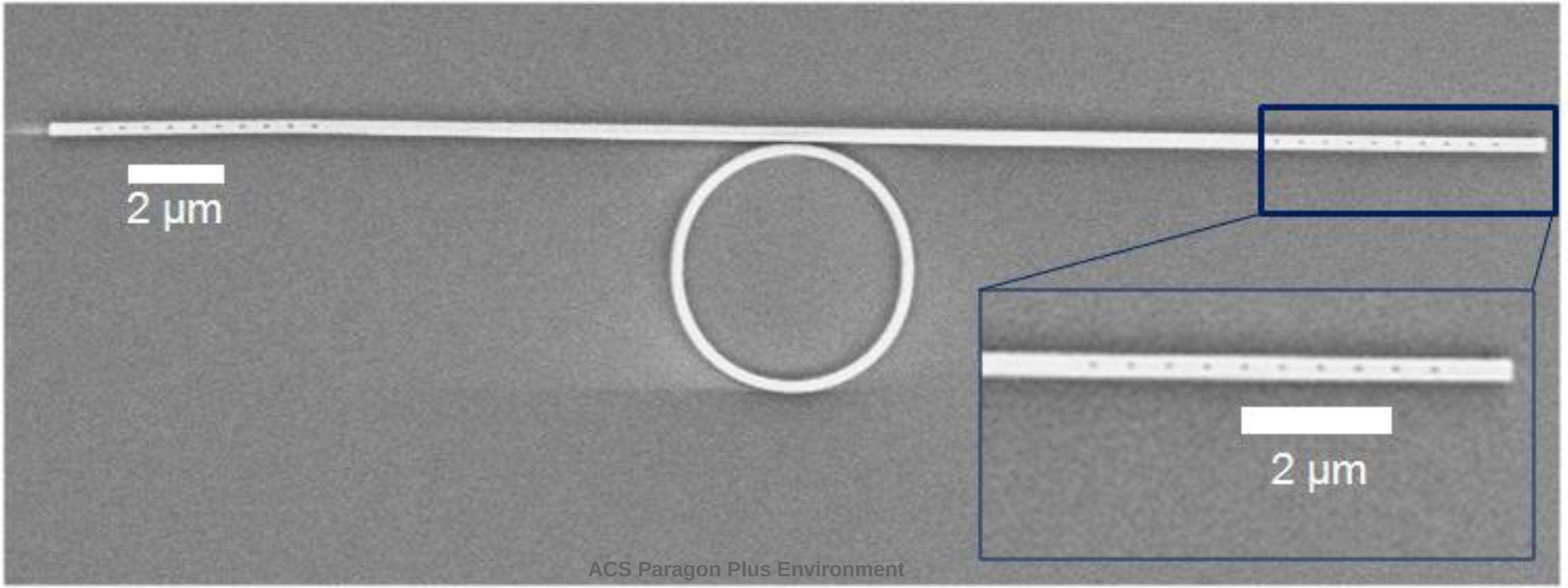
(a)
2 μm
2 μm
ACS Paragon Plus Environment

(b)